RESEARCH ARTICLE

Proteomic analysis identified N-cadherin, clusterin, and HSP27 as mediators of SPARC (secreted protein, acidic and rich in cysteines) activity in melanoma cells

María Soledad Sosa[1,**], María Romina Girotti[1*], Edgardo Salvatierra[1], Federico Prada[1], Juan Antonio López de Olmo[2***], Silvia Juárez Gallango[2], Juan Pablo Albar[2], Osvaldo Luis Podhajcer[1] and Andrea Sabina Llera[1]*

[1] Laboratory of Molecular and Cellular Therapy, Fundación Instituto Leloir-CONICET and Facultad de Ciencias Exactas y Naturales, Universidad de Buenos Aires, Buenos Aires, Argentina
[2] Proteomics Unit, Centro Nacional de Biotecnología (CNB), Madrid, Spain

Received: March 15, 2007
Revised: July 24, 2007
Accepted: August 10, 2007

Secreted protein, acidic and rich in cysteines (SPARC) is a secreted protein associated with increased aggressiveness of different human cancer types. In order to identify downstream mediators of SPARC activity, we performed a 2-DE proteomic analysis of human melanoma cells following antisense-mediated downregulation of SPARC expression. We found 23/504 differential spots, 15 of which were identified by peptide fingerprinting analysis. Three of the differential proteins (N-cadherin (N-CAD), clusterin (CLU), and HSP27) were validated by immunoblotting, confirming decreased levels of N-CAD and CLU and increased amounts of HSP27 in conditioned media of cells with diminished SPARC expression. Furthermore, transient knock down of SPARC expression in melanoma cells following adenoviral-mediated transfer of antisense RNA confirmed these changes. We next developed two different RNAs against SPARC that were able to inhibit *in vivo* melanoma cell growth. Immunoblotting of the secreted fraction of RNAi-transfected melanoma cells confirmed that downregulation of SPARC expression promoted decreased levels of N-CAD and CLU and increased secretion of HSP27. Transient re-expression of SPARC in SPARC-downregulated cells reverted extracellular N-CAD, CLU, and HSP27 to levels similar to those in the control. These results constitute the first evidence that SPARC, N-CAD, CLU, and HSP27 converge in a unique molecular network in melanoma cells.

Keywords:
Melanoma / Osteonectin / Secreted protein / SPARC / Two-dimensional gel electrophoresis

1 Introduction

Secreted protein, acidic and rich in cysteine (SPARC), also named osteonectin or BM40, is a glycoprotein that belongs to the family of matricellular proteins [1]. SPARC is expressed during embryonic development in cartilage and bone while in the normal adult, expression of SPARC is limited to tissues involved in repair and remodeling, such as wound healing processes [2]. In fibroblasts and endothelial cells, SPARC acts generally as a cell cycle inhibitor that arrests cells in mid-G1, delaying progression to S-phase [3–5]. SPARC has also been described as a de-adhesive protein, as it inhibits cell spreading and induces cell rounding in certain

Correspondence: Dr. Andrea Sabina Llera, Fundación Instituto Leloir, Av. Patricias Argentinas 435, 1405BWE Buenos Aires, Argentina
E-mail: allera@leloir.org.ar
Fax: +54-11-5238-7501

Abbreviations: ANOVA, analysis of variance; **CLU,** clusterin; **N-CAD,** N-cadherin; **SPARC,** secreted protein, acidic and rich in cysteines

* Both authors contributed equally to this work
** Current address: Department of Pharmacology, University of Pennsylvania School of Medicine, Philadelphia, USA
*** Current address: Proteomics Unit, Centro Nacional de Investigaciones Cardiovasculares (CNIC), Madrid, Spain

cell types, disruption of focal adhesion complexes, and reorganization of actin stress fibers [6], at least in part through direct interaction with integrin-linked kinase [7]. Interestingly, pathologies such as cancer where there is a misbalance in cell attachment, growth, and/or invasive capacity are characterized in general by abnormally elevated SPARC expression [8]. In fact, in recent years, SPARC has been described as a marker of malignancy in several cancer lineages [1]. Elevated levels of SPARC in human cancer originate either in malignant cells themselves or in associated stromal cells, depending on the cancer type. In those of ectodermal origin (such as melanoma and glioma) malignant cells express elevated levels of SPARC [9, 10]. In contrast, in several adenocarcinomas, SPARC is mainly produced by stromal cells [11], while its expression in malignant cells is thought to be repressed by promoter hypermethylation [12]. This lineage-dependent heterogeneity in SPARC production may account for the apparently contradictory effects of SPARC in different cancer lineages. For example, SPARC expression by melanoma and glioma cells has been linked to an aggressive phenotype *in vivo* [10, 13]. Moreover, soluble SPARC has been shown to promote migration of malignant cells and chemotaxis to bone extracts indicating that SPARC might promote metastatic dissemination [14, 15]. In contrast, ectopic overexpression of SPARC in ovarian carcinoma cells led to increased tumor cell apoptosis, and inhibition of *in vivo* tumor growth [16, 17]. In addition, SPARC was shown to inhibit neuroblastoma *in vivo* growth through the inhibition of tumor-associated angiogenesis [18]. Our own studies have demonstrated that knock down of SPARC expression in human melanoma cells obliterated *in vivo* tumor growth through a mechanism that involved the activation of polymorphonuclear cell antitumoral activity [13, 19]. Indeed, we demonstrated that IIB-MEL-LES-derived human melanoma cell line L-CMV generated solid tumors in nude mice, while its counterpart with 80% lower SPARC expression, the cell clone L-1D, was completely unable to grow as solid tumor *in vivo*. In addition, downregulation of SPARC expression greatly impaired melanoma cell migration and invasive capacity suggesting that different effectors might mediate the diversity of SPARC pro-tumorigenic effects [13].

Thus, SPARC seems to be involved in tumor progression through different molecular mechanisms depending on the tumor lineage. While some of these effects might be directly ascribed to SPARC, it is still unclear whether part of SPARC effects might be related to downstream effectors of the protein, acting on the malignant cells themselves or adjacent stromal cells. We envisioned that a proteomic analysis of proteins released to the extracellular medium (secretome) following modulation of SPARC expression in melanoma cells might provide clues on the potential molecular mediators and mechanisms by which this protein might act. By using a proteomics approach and three different strategies to knock down SPARC expression, we identified N-cadherin (N-CAD), clusterin (CLU), and HSP27 as potential downstream mediators of SPARC tumorigenic effects in melanoma cells.

2 Materials and methods

2.1 Cell culture

Melanoma cell lines and clones were grown in DMEM/F12 containing no transferrin or epidermal growth factor, and supplemented with 10% v/v FBS and antibiotics. L-1D and L-CMV cells were obtained as described in [13]. Briefly, human melanoma cell line IIB-MEL-LES [20] were transfected with Rc/CMV vector (Invitrogen, San Diego, CA) carrying SPARC full-length cDNA cloned in antisense orientation. Clone L-1D was derived from the stably transfected bulk culture by limited dilution. The control L-CMV cell line was generated by stable transfection of IIB-MEL-LES cells with an empty Rc/CMV vector. Both L-CMV and L-1D cells were thawed from original stocks, selected in G418 and routinely checked for SPARC production. All cells were maintained in culture for no longer than five passages.

2.2 Preparation of human melanoma conditioned media

Cells were seeded according to similar percentages of confluency. Taking into account differences in spreading between L-CMV and L-1D, 5×10^6 L-CMV and 3.5×10^6 L-1D cells were seeded in 150 mm plates, grown for 24 h in serum-containing medium, washed three times with PBS and kept in serum-free medium for additional 24 h. Media were collected and cleared by centrifugation. Resulting supernatants were supplemented with 0.01 μM aprotinine, 1 μM leupeptin, 130 μM bestatin, 1 μM pepstatin, 1 mM PMSF, and 0.14 μM E-64, and concentrated 60-fold in a Centriprep-3 (Millipore, Billerica, MA). Proteins were precipitated with 10% v/v TCA/acetone and the resulting pellet was solubilized in lysis buffer (7 M urea, 4% w/v, CHAPS, 2 M thiourea, 2 mM TCEP-HCl, 0.5% v/v IPG buffer range 3–10) by shaking during 2 h at room temperature. Protein concentration was assessed with 2D-Quant Kit (GE Healthcare, Piscataway, NJ).

2.3 2-DE

2-DE was performed as described in [21], with minor modifications. Briefly, samples (60 μg total protein) were diluted in rehydration solution (7 M urea, 2 M thiourea, 2% w/v CHAPS, 0.5% v/v IPG buffer range 3–10, 50 mM DTT) and applied by in-gel rehydration into 18 cm, pH 4–7 IPG strips (GE Healthcare). IEF was performed in an Ettan IPGphor system (GE Healthcare) according to manufacturer's instructions. After IEF, strips were incubated for 15 min in equilibration buffer (50 mM Tris-HCl, 6 M urea, 30% v/v glycerol, 2% w/v SDS, 0.005% w/v bromophenol blue) containing 1% w/v DTT, followed by a second 15 min-incubation with 4% w/v iodoacetamide in equilibration buffer. Second dimension (SDS-PAGE) was performed in a four-gel array using a Hoefer 660 electrophoresis unit (GE Health-

care). IPG strip ends were clipped to fit gel width and loaded into 18×16 cm^2 12.5% SDS-polyacrylamide gels. After the run, spots were detected using MS-compatible silver nitrate staining [22].

2.4 Data analysis and statistics of 2-DE data

Silver-stained gels were scanned in an image scanner and analyzed with ImageMaster 2D Elite 3.10 software (both from GE Healthcare). Spots were automatically detected, manually edited, and matched between gels. Spot volumes were then normalized to the sum of volumes of spots present in all gels. Normalized volumes for technical replicates were averaged. Statistic significance of differences between average spot volumes in each condition was estimated using Welch-modified Student's *t*-test, and Wilcoxon's rank sum test. Normalization and inference statistics were performed under R-System V2.1.1 (R Development Core Team. 2005. R: A language and environment for statistical computing. Vienna, Austria: R Foundation for Statistical Computing).

2.5 In-gel digestion and peptide mass fingerprint by MALDI-TOF MS

In-gel tryptic digestion of differential 2-DE spots was automatically performed in an Investigator ProGest unit (Genomic Solutions, Cambridgeshire, UK), according to Shevchenko *et al.* [23], with some modifications. Protein spots were excised from silver stained gels and washed once with Milli-Q water and twice with 50% ACN for 15 min. Gel pieces were washed with a 1:1 solution of 0.1 M NH_4HCO_3 and ACN for 15 min and then incubated in 10 mM DTT/0.1 M NH_4HCO_3 for 30 min at 56°C followed by incubation in 55 mM iodoacetamide/0.1 M NH_4HCO_3 for 20 min at room temperature. Supernatants were discarded and gel pieces were washed with 100 μL NH_4HCO_3, followed by two washes with 100 μL of 25 mM NH_4HCO_3 in 50% ACN. Supernatants were again discarded and gel pieces were rehydrated with trypsin digestion buffer (50 mM NH_4HCO_3, 5 mM $CaCl_2$). For trypsin digestion, 10 ng/μL of modified porcine trypsin (Promega, Madison, USA) were added in a final volume of 20 μL. Gel pieces were incubated at 4°C for 45 min, after which 25 mM NH_4HCO_3 was added, and tubes were further incubated overnight at 37°C. The supernatant was transferred into a clean tube and the residual gel pieces were extracted twice in 50% ACN and 0.5% TFA. Supernatant and extracts were pooled into one tube, dried by vacuum centrifugation and reconstituted in 10 μL of 0.1% v/v TFA in 33% v/v aqueous ACN. Subsequently, the digested mixture (0.4 μL) were mixed with equal volume of CHCA (0.3 mg/mL in 30% ACN, 0.1% TFA).

A 0.4 μL-aliquot of each peptide mixture was deposited onto an AnchorChip MALDI target (Bruker Daltonics, Bremen, Germany) and allowed to dry at room temperature. Peptide spectra were obtained on a Reflex IV MALDI-TOF mass spectrometer (Bruker Daltonics) equipped with a SCOUT source in positive-ion reflector mode. Ion acceleration voltage was set at 25 kV. Spectra were processed using Xtof 5.1.1 software that analyses raw XMASS data generated by FLEXControl 1.1 (Bruker Daltonics). For peak list generation, each spectrum was processed by subtracting the baseline and then internally calibrating using trypsin autoproteolysis signals, specifically 842.510 and 2211.105 Da peptides, in the 800–2600 m/z range. For protein identification, the nonredundant NCBI database was searched using MASCOT 2.1 (www.matrixscience.com) through the BioTools 2.1 interface provided by Bruker Daltonics (see versions in Table 1). Search parameters were set as follows: carbamidomethyl cysteine as fixed modification, oxidized methionine as variable modification, peptide mass tolerance 80 ppm and one missed trypsin cleavage site.

2.6 Immunoblotting analysis

Protein samples were separated in a 12% SDS-polyacrylamide gel and transferred onto PVDF membranes using a Trans-blot apparatus (BioRad, Hercules, CA). Total protein staining on transferred membranes (with Ponceau S) and on a gel run in parallel and stained with Sypro Ruby were used to control for uniform loading. Membranes were blocked with 5% w/v skim milk in PBS with 0.05% v/v Tween 20 and incubated for 2 h in appropriate dilutions of mouse monoclonal anti-SPARC antibody AON-1 (hybridoma purchased to Developmental Studies Hybridoma Bank, Iowa City, IA) or the following polyclonal antibodies: rabbit anti-N-CAD (H-63 Santa Cruz Biotechnology, Santa Cruz, CA), rabbit anti-CLU (H-330 Santa Cruz Biotechnology), and mouse anti-HSP27 (F-4 Santa Cruz Biotechnology). After extensive washing, membranes were incubated with peroxidase-conjugated AffiniPure Goat antimouse IgG (1:2500, Jackson Immunoresearch Laboratories) or peroxidase-conjugated AffiniPure goat anti-rabbit IgG (1:1700, Jackson Immunoresearch Laboratories) for 45 min, and washed before detection by ECL chemiluminescence (GE Healthcare). OD of bands was measured using Image J (Rasband WS. Image J. Bethesda, Maryland, USA: U. S. National Institutes of Health). Values were normalized according to total protein loading and expressed as percentage of the density corresponding to the control cell line. The Student's *t*-test (in the case of comparison of two samples) and the unpaired analysis of variance (ANOVA) test with Dunnett post-test (for three-way comparisons) were used for calculation of statistical significance.

2.7 Flow cytometry

For flow cytometry analysis, L-CMV and L-1D cells grown for 24 h in medium supplemented with 10% v/v FBS were washed and detached with 1.25 mM EDTA in PBS. After washing with ice-cold medium, cells were initially incubated with 10% v/v goat normal serum in PBA (PBS, 5 mg/mL BSA, 0.01% w/v sodium azide) for 30 min followed by additional 30 min incubation with a 2 μg/mL of monoclonal anti-

N-CAD antibody (anti-A-CAM, clone CG-4, Sigma, St. Louis, MO). Cells were washed twice with PBA and fixed in 4% w/v paraformaldehyde in PBS for 10 min at room temperature. After washing with PBA, samples were incubated for 30 min with a secondary goat antimouse IgG antibody conjugated to Alexa Fluor 488 (Molecular Probes, Eugene, OR) diluted in PBA (at 2 μg/mL). Cells were extensively washed, resuspended in PBS and subjected to flow cytometry using a FACStar Plus flow cytometer (BD Biosciences, San Jose, CA). Unless otherwise specified, all steps were performed at 4°C.

2.8 Immunofluorescence

For immunofluorescence assay, L-CMV and L-1D cells were seeded in cover slides and grown as described above. After 48 h, cells were washed twice with PBS, fixed in 4% w/v paraformaldehyde, washed four times with PBS, blocked with 1% v/v donkey serum in PBS for 1 h, and incubated overnight with rabbit anti-N-CAD antibody (H-63, Santa Cruz Biotechnology) diluted 1:50 in blocking solution. After this step, cells were washed twice with PBS and incubated for 2 h in Cy2-conjugated donkey antirabbit antibody in a 1:200 dilution in PBS (Jackson Immunoresearch, West Grove, PA). Samples were washed with 0.01% v/v Tween-20 containing PBS and then incubated for 10 min with 10 mM Hoescht 33258 in PBS to stain nuclei. After washing, slides were mounted with Fluorsave (Calbiochem, EMD Biosciences, La Jolla, CA) and evaluated by a LSM 510 confocal microscopy (Carl Zeiss, Göttingen, Germany).

2.9 Studies with adenoviral vectors

Adenovirus carrying SPARC cDNA in sense orientation (Ad-SPs), antisense orientation (Ad-SPas), or βgal (Ad-βgal) were obtained as described in [19]. Concentration of recombinant vectors was expressed as 50% tissue culture infective dose *per* milliliter on HEK 293 cells (TCID50/mL) [24]. For preparation of conditioned media and cell transduction, 2.5×10^5 L-CMV and 2.0×10^5 L-1D cells were seeded in 35 mm plates and grown in serum-containing medium as described above. After 24 h, cell transduction was carried out using 1×10^9 $TCID_{50}$/mL during 6 h in serum-free medium. Cells were then kept in 10% v/v FBS-supplemented culture medium for 18 h, washed three times with PBS, and kept in serum-free medium for additional 24 h. Conditioned media were supplemented with the previously described protease inhibitor cocktail. Protein concentration was performed using the Nano Orange Kit (Molecular Probes).

2.10 RNAi design, construction, and stable transfection of melanoma cells

A DNA vector-based siRNA was designed to stably knock down the expression of SPARC in melanoma cell lines. Design of specific siRNA was done using GenScript Target Finder (www.genscript.com/ssl-bin/app/rnai). BLAST search was used for selecting two target noncrossmatching sequences among the siRNA candidates generated. The 21-nucleotide target sequences starting at base 321 (5′- CCA-GAACCACCACTGCAAAC-3′) and base 2175 (5′-TCTT-AGTCTTAGTCACCTTAT-3′) of the human SPARC mRNA were ordered as siRNA expression cassettes with a human U6 promoter. For cloning into an expression vector, a version of pcDNA6-V5-His-B vector (Invitrogen, Carlsbead, MA) lacking the CMV promoter was generated by digestion with *Nhe*I and *Bgl*II, complete filling in and relegation, and named pBLAST. Each siRNA cassette was digested and cloned into *Mlu*I and *Hin*dIII sites of pBLAST. The resulting siRNA vectors were named pSP321 and pSP2175.

Vectors pSP2175, pSP321, and pBlast were transfected into human melanoma cells using Lipofectamine 2000 (Invitrogen) according to manufacturer's recommendations. Briefly, cells at 85% confluence in 24-well plates were transfected with a mixture of 1 μg plasmid and 3 μL Lipofectamine 2000. Thirty-six hours after transfection, cells were seeded at a 1:10 dilution into fresh growth medium supplemented with 1 μg/mL of blasticidin and allowed to grow for at least three passages in selective medium. In this way, L-2175, L-321, and LBLAST cell lines were generated. To evaluate the stable knockdown of SPARC expression, 1 μg of total protein obtained from 24 h-conditioned serum-free medium from each transfection were used in immunoblotting analysis with an anti-SPARC antibody (see above). Isolation of stable individual clones with downregulated SPARC expression was carried out by limiting dilution of cell lines L-2175 and L-321 using 1–5 μg/mL blasticidin in culture medium. Clones L2F6 (from L-2175 cells) and L3B9 (from L-321 cells), with different degrees of SPARC downregulation, were routinely maintained in selective media during further studies.

2.11 Northern blot analysis

Total RNA was extracted from LBLAST, L2F6, and L3B9 cells using Tri Reagent (Sigma) and a standard protocol [25]. Fifteen micrograms aliquots were subjected to electrophoresis on 1% w/v agarose, 18% v/v formaldehyde, 1X MOPS gels and transferred to Hybond-N+ nylon membranes (GE Healthcare) overnight in 20X SSC according to standard upward capillary blot procedure. Following prehybridization in 1% w/v bSA, 0.5 M phosphate buffer, pH 7.4, 1 mM EDTA, 7% w/v SDS, the RNA blots were hybridized with a SPARC cDNA probe labeled with (^{32}P)-dCTP by random primer labeling. The membranes were rehybridized with a 36B4 cDNA probe for normalization of loading levels. Gene expression levels of SPARC were quantified by densitometry of bands and normalized against 36B4.

2.12 *In vivo* assays

Eight to ten weeks old athymic N:NIH(S)-nu mice, received s.c. inocula of 5×10^6 melanoma cells (either LBLAST, L2F6,

or L3B9) in the left flank, in a total volume of 100μL. Perpendicular diameters were used to determine tumor volume, as $d1^2 \times d2/2$, where *d1* is the smaller diameter and *d2* is the larger one. Surviving mice were followed for 2 months and those harboring tumors greater than 2 cm^3 were euthanized following institutional guidelines approved by NIH authorities.

3 Results

3.1 Secretome analysis of cell lines with differential SPARC expression reveals SPARC-regulated proteins

Conditioned media were obtained from the human melanoma cell clone L-1D expressing around 20% of the amount of SPARC expressed by control cells due to the stable expression of SPARC-antisense RNA. These conditioned media were compared with conditioned media obtained form control melanoma cells stably transfected with the empty vector (see Section 2 for details).

A set of four analytical gels, each with 60 μg of total protein precipitated from independently conditioned media (biological replicates), was run for each condition analyzed (L-CMV and L-1D). An average of 598 protein spots in each L-CMV gel (range 470–757) and 564 spots in each L-1D gel (range 470–633) were detected and matched, and spot volumes were normalized to the sum of volumes of all matched spots on the gel (504 spots). Normalized volumes for individual spots were then averaged over replicates and differences in averaged normalized volumes were statistically analyzed as described in Section 2. Twenty-three spots were selected as differential ($p<0.05$) between L-CMV and L-1D using a Student *t*-test (Fig. 1 and Table 1). Seven of these 23 spots were also significantly different according to the nonparametric Wilcoxon test (Table 1). Peptide fingerprinting analysis of the 23 differential spots resulted in a total of 15 reliable identifications of 12 proteins, including SPARC. Table 1 summarizes 2-DE and MS data obtained for the differential spots. One remarkable finding was the differential levels of collagens I and V in SPARC-downregulated cells. As it is thoroughly established that SPARC regulates collagen levels and assembly [26, 27], our results render our experimental approach as valid to detect differences in expression levels of SPARC-regulated proteins.

From the differential spots listed in Table 1, we selected for technical validation three putative SPARC targets: N-CAD, CLU and HSP27. Secretion of N-CAD and CLU was significantly diminished following stable knock down of SPARC expression; under the same conditions, we observed increased levels of secreted HSP27 (Fig. 2A). In order to technically validate these differences we performed an immunoblotting analysis using specific antibodies on three independent preparations of conditioned media. Densitometric analysis confirmed the diminished secretion of N-CAD and CLU (Fig. 2B). Accordingly, galectin-1, whose spots were not statistically significant by 2-DE analysis, was also

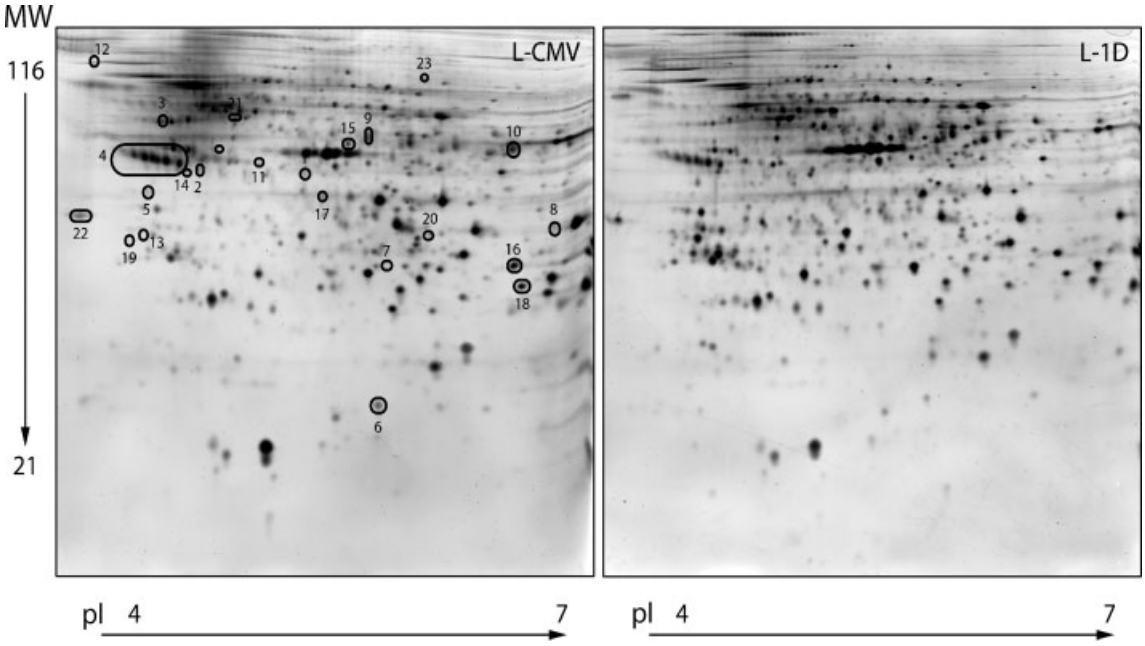

Figure 1. Differential secretome analysis of melanoma cells with modulated SPARC expression levels. Representative 2-D gels from conditioned media of L-CMV (left) and L-1D (right) in a pH range 4–7, stained with silver nitrate. Differential spots (*t*-test $p<0.05$) are indicated in boxes numbered as in Table 1.

Table 1. List of differential spots in the secretome of L-CMV and L-1D human melanoma cells with modulated SPARC activity

Spot No.[a]	Acc. no. (gi)[b]	Protein identification	Log2 Fold Change[b]	Theoretical *M*r (x10-3)/p*I*	*p* (Student-*t*)	*p* (Wilcoxon)	MASCOT[c]	% Pept. coverage[d]	M|U peptides[e]
1	178855	CLU, β chain	−3.1	26/5.2	0.0471	NS	73	20	5|9
2	178855	CLU, α chain	−2.0	23/8.2	0.0424	NS	94	36	5|0
3	51105874	Secernin 1	−3.0	47/4.4	0.0170	NS	134	22	7|1
4	4507171	SPARC	−1.8	33/4.7	0.0181	NS	160	49	9|1
5	38014150	Collagen, type V, α 1 chain	−1.7	59/4.9	0.0228	0.0286	96	14	6|1
6	253483	N-CAD	−1.5	100/4.6	0.0089	0.0286	80	10	6|1
7		N/I	−1.4		0.0103	NS			
8		N/I	−1.3		0.0110	0.0286			
9	37790800	Renin, chain B	−1.0	45/6.7	0.0177	0.0286	145	25	9|3
10	37790800	Renin	−0.6	45/6.1	0.0414	NS	179	15	6|2
11	7428712	Cytokeratin I, type II	−1.0	66/6.0	0.0439	NS	104	13	5|1
12		N/I	−2.8		0.0243	NS			
13		N/I	−1.3		0.0485	NS			
14		N/I	−2.4		0.0132	NS			
15	14250401	β-actin	0.7	41/4.9	0.0158	NS	125	22	4|1
16	662841	HSP27	1.1	22/7.8	0.0283	0.0286	79[f]	22	3|0
17	2388555	Collagen, type I, α-2 chain	1.3	112/9.0	0.0347	0.0286	75	8	6|0
18	14250063	Peroxiredoxin 3	1.3	28/7.1	0.0280	NS	73	26	6|16
19		N/I	1.6		0.0075	0.0286			
20		N/I	1.7		0.0375	NS			
21	567053	β-5 tubulin	1.9	50/4.5	0.0040	NS	181	27	11|2
22	4930075	p32, chain C	2.0	24/4.1	0.0390	NS	89	30	4|0
23		N/I	3.2		0.0062	NS			

a) Spot numbers correspond with the gel image in Fig. 1.

b) Fold-change is expressed as base 2 logarithmic ratios, that is, log 2 (L-1D/L-CMV). As a reference, a two-fold increase in L-1D respect to L-CMV corresponds to a value of 1 in the table, whereas a two-fold decrease in L-1D respect to L-CMV corresponds to –1 in the table.

c) MASCOT score correspond to MOWSE score as informed by MASCOT. The following NrNCBI database versions were used: 20030816, 20040324, 20041019.

d) % pept. cov.: percent coverage of peptide sequence. Note that some identifications correspond to fragments of smaller size than the expected length of the protein sequence deposited in NCBI data bank; however, % of sequence coverage was calculated using the complete deposited sequence for standardization purposes. It is expected, then, that some identified spots have higher % of real coverage (*i.e.*, spots 5, 6, 11, 17).

e) M|U peptides: matched|unmatched peptides.

f) For this spot additional MS/MS information has been obtained in a MALDI TOF/TOF instrument (Ultraflex, Bruker; courtesy Emilio Camafeita, CNIC, Madrid), with the following results: MASCOT fragmentation score 126; sequence of the 1163 Da fragmented peptide: LFDQAFGLPR; number of assigned/total peptides in fragmentation spectrum: 28/104.

N/I, not identified; NS, not significant in statistical tests alternative to Student *t*-test ($p>0.05$). Validated proteins are shadowed in gray.

not significantly different by immunoblotting analysis (not shown). Real-time PCR experiments indicate that changes in extracellular protein levels are not always correlated with mRNA levels of these proteins (Fig. 1 of Supporting Information).

3.2 Membrane N-CAD is also differentially expressed in L-1D and L-CMV cells

The form of N-CAD that was found differential in 2-D gels had a molecular weight of 24 kDa and corresponded to a fragment of the extracellular domain of N-CAD (Fig. 2 of Supporting Information). However, immunoblotting using an anti-N-CAD polyclonal antiserum failed to detect this low molecular weight form. Instead, a 90 kDa fragment, corresponding to the complete extracellular domain, was detected as differential by this antibody. Previous work has shown that N-CAD extracellular domain is susceptible to specific cleavage by ADAM-10 metalloprotease ([28], see Section 4), releasing a soluble form of N-CAD that retains adhesive and neurite-promoting function [29, 30]. In order to see if differential levels of N-CAD in these cell types were restricted to its soluble form or, in contrast, reflect an overall regulation of N-CAD expression, we assessed whether the differences in secreted N-CAD levels correlated with differences in expression levels of membrane N-CAD. Flow cytometry analysis

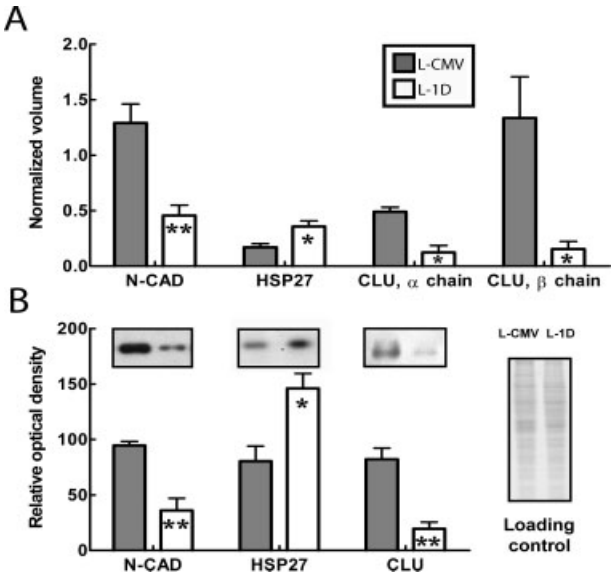

Figure 2. Relative quantitative comparison among 2-DE and immunoblotting data for the validated proteins N-CAD, HSP27, and CLU in L-1D and L-CMV conditioned media. (A) Normalized volume of spots in scanned 2D-gels. CLU, a heterodimer, rendered two differential spots corresponding to its different monomers, α and β. Data shown represent the average of four biological replicates. (B) Relative optical densities of scanned immunoblotting bands. Values were first normalized to optical densities corresponding to total protein loading, as evaluated by a parallel gel stained with Sypro Ruby. Data shown represent the average of three biological replicates. A representative immunoblot image is shown for each protein, along with a representative loading control of total protein stained with Sypro Ruby. Asterisks indicate statistically significant differences (*: *t*-test $p<0.05$; **: *t*-test $p<0.01$).

showed decreased N-CAD cell surface expression levels in L-1D cells compared to control L-CMV cells (Fig. 3A). Moreover, confocal microscopy demonstrated a decrease in the overall fluorescent intensity specific for N-CAD in L-1D cells respect to L-CMV cells (Fig. 3B). In addition, immunoblotting analysis of cell extracts also showed lower levels of a band of 113 kDa (corresponding to the size of the membrane-associated form of N-CAD) in L-1D cells compared with L-CMV cells (not shown).

3.3 Re-expression of SPARC in L-1D clone restores levels of extracellular N-CAD, CLU and HSP27

In order to further confirm that SPARC was responsible for the changes in the secreted levels of the three proteins, we transiently re-expressed SPARC in L-1D cells following adenovirus-mediated transfer of its full-length cDNA in the sense orientation. Seventy-two hours after viral transduction, levels of extracellular N-CAD, CLU, and HSP27 were partially restored to those seen in control L-CMV cells, as evaluated by immunoblotting (numbers below bands correspond to the percentage of OD considering L-CMV as 100%), concomitantly with an increase in SPARC production (Fig. 4). Transduction of melanoma cells with control virus carrying β-galactosidase led to low to moderate increases in SPARC expression, a finding consistently observed regardless of whether the control adenovirus expressed β-gal or another nonrelated gene such as CRE [31].

3.4 Changes in N-CAD, CLU, and HSP27 levels upon adenovirus-mediated transfer of SPARC antisense RNA

In order to confirm that extracellular levels of N-CAD, CLU, and HSP27 are under direct regulation of SPARC we transiently transduced IIB-MEL-LES melanoma cells with an adenovirus expressing SPARC antisense RNA (Ad-SPas). Using adenovirus-expressing β-galactosidase (Ad-βgal) as control, we showed a decrease of 40% in the levels of SPARC at 72 h after transduction with Ad-Spas (Fig. 5A). This transient knock down of SPARC expression in IIB-MEL-LES cells led to a reduction in the secreted levels of N-CAD and CLU,

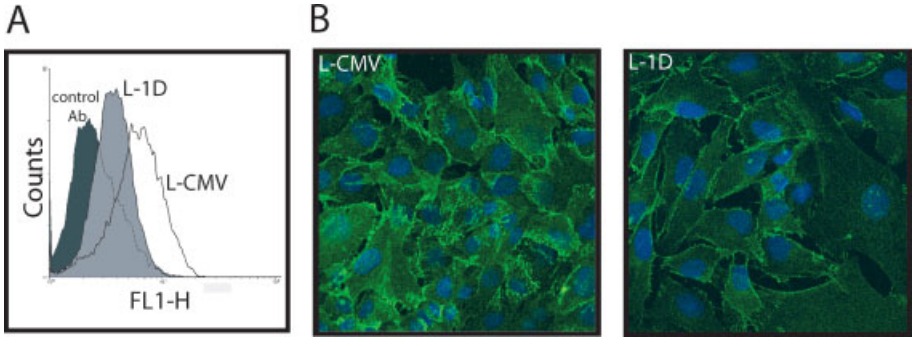

Figure 3. Flow cytometry and immunofluorescence analysis of membrane-bound N-CAD expressed in L-1D and L-CMV cells. (A) Flow cytometry analysis of L-CMV (clear profile) and L-1D (light gray profile) cells stained with anti-N-CAD antibody. Dark gray profile shows L-CMV and L-1D cells probed with isotypic control antibody. L-1D cells show lower levels of total N-CAD staining.(B) Immunofluorescence specific for N-CAD (green) in L-CMV and L-1D cells. Confocal microscopy photographs demonstrate a decrease in the overall fluorescent intensity in L-1D cells compared with L-CMV cells. Cell nuclei were stained with Hoescht 33258 (blue).

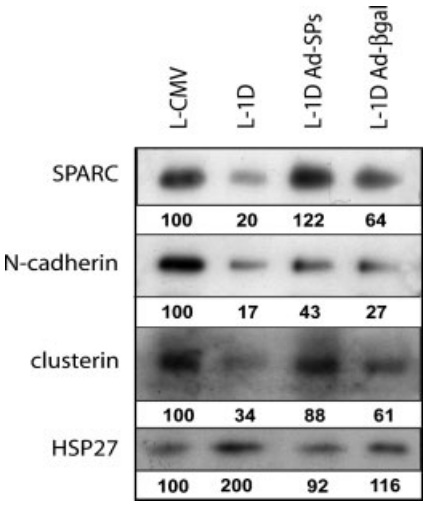

Figure 4. Immunoblotting detection of extracellular N-CAD, CLU and HSP27 during transient re-expression of SPARC in L-1D clone. L-1D clone was infected with adenoviruses expressing SPARC sense sequence (L-1D Ad-SPs) or control β-galactosidase (L-1D Ad-βgal). AdSPs rescued SPARC expression to that in L-CMV. Expression of extracellular N-CAD, CLU, and HSP27 was restored to levels close to those seen in control L-CMV cells. Numbers below each band correspond to the percentage of OD, normalized by total protein loading, and relative to L-CMV cells (100%).

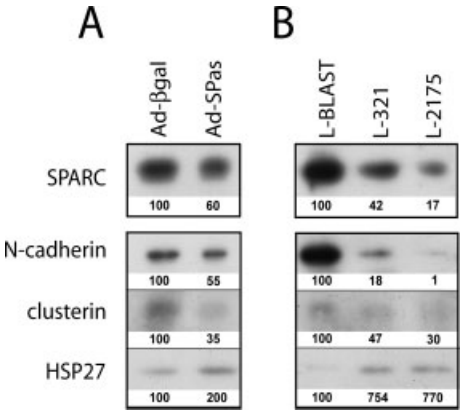

Figure 5. Immunoblotting detection of CLU, N-CAD and HSP27 in conditioned media of IIB-MEL-LES cells treated with transient or stable molecular tools used for downregulation of SPARC expression. (A) IIB-MEL-LES cells were infected with adenoviruses expressing SPARC antisense sequence (Ad-SPas) or control β-galactosidase (Ad-βgal). The transiently induced partial inhibition of SPARC expression promotes similar changes to those seen in L-1D and L-CMV cells in the expression of the selected proteins. (B) IIB-MEL-LES cells were transfected with two different siRNA-expressing vectors, named 2175 and 321, to stably knock down expression of SPARC. L-2175, L-321, and L-BLAST (control) cell lines confirm the expression differences observed in IIB-MEL-LES-derived L-1D clone and L-CMV cell line. Numbers below each band correspond to the percentage of OD, normalized by total protein loading, relative to L-CMV cells (100%).

respectively and an increase in the secreted levels of HSP27. This evidence is consistent with a SPARC-specific effect on the regulation of N-CAD, CLU, and HSP27 extracellular levels.

3.5 Two SPARC RNAi that block the *in vivo* melanoma tumorigenicity confirmed the changes in the levels of N-CAD, CLU, and HSP27

In order to further confirm that N-CAD, CLU, and HSP-27 are potential mediators of SPARC, IIB-MEL-LES melanoma cells were transfected with two different RNAis and selected for 12 days in the presence of blasticidin. We confirmed that L-321 and L-2175 RNAi expression led to an average of 40 and 60% decreases, respectively, in SPARC mRNA expression levels compared to control L-BLAST cells as assessed by real time PCR (data not shown). This decrease in SPARC mRNA expression was confirmed by immunoblotting of the secreted protein (Fig. 5B). Confirming the previous data, expression of both RNAis induced a decrease in the levels of secreted N-CAD and CLU, with a simultaneous increase in HSP27 secreted levels (Fig. 5B).

We finally isolated two different stable cell clones (L3B9 and L2F6) that were derived from L-321 and L-2175 RNAi-transfected bulk cell cultures, respectively. Northern blot analysis demonstrates a strong decrease in the expression levels of both mRNA forms of SPARC in L2F6, while L3B9 showed a moderate decrease compared to control cells (Fig. 6A). This decrease in SPARC mRNA levels was confirmed by immunoblotting of the secreted protein (see Fig. 6C, left panel). Although there was no strict correlation with SPARC levels, immunoblotting analysis confirmed that downregulation of SPARC expression in L2F6 and L3B9 cell clones promoted a decrease in N-CAD and CLU secreted levels (Fig. 6C, center panels). Levels of extracellular HSP27, however, did not show statistically significant differences in LBLAST, L2F6, and L3B9 conditioned medium (Fig. 6C, right panel).

In previous studies, we have shown that stable or transient knock down of SPARC expression using SPARC antisense RNA inhibited the *in vivo* tumorigenicity of human melanoma cells in nude mice [13]. In order to establish if the expression of the RNAs might have the same effect we injected nude mice with tumorigenic inocula of L2F6 and L3B9. In accordance with our previous results, knock down of SPARC expression in L3B9 and L2F6 clones strongly inhibited or completely obliterated, respectively, their *in vivo* tumorigenic capacity, confirming the protumorigenic role of SPARC in human melanoma cells (Fig. 6B).

4 Discussion

The present study demonstrates that knock down of SPARC expression in human melanoma cells induced a clear reduction in the levels of secreted N-CAD and CLU and increased

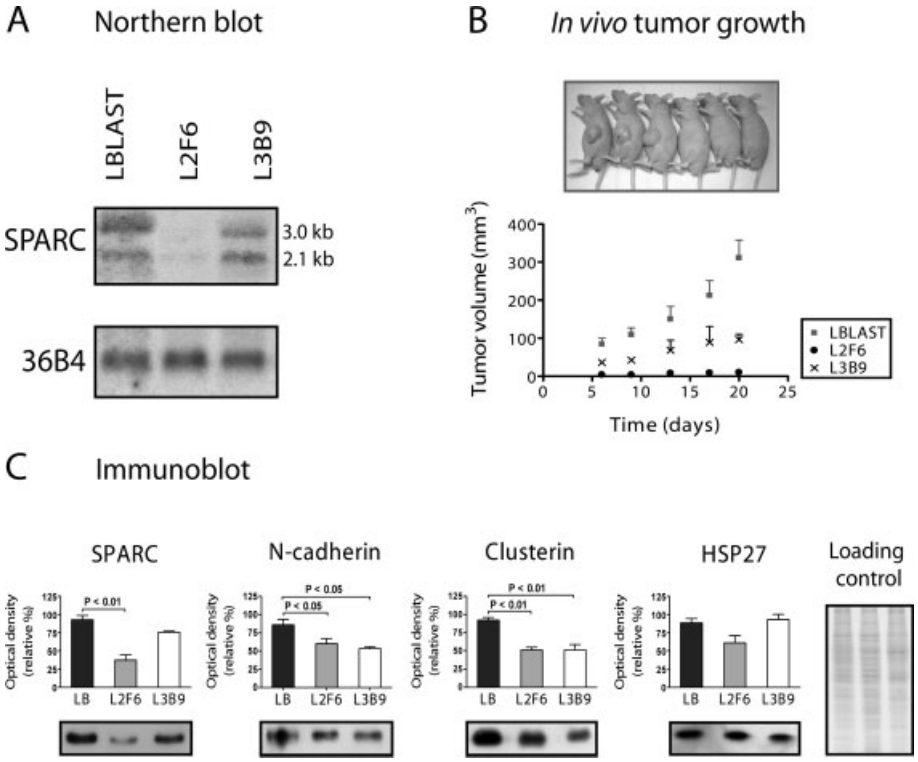

Figure 6. *In vitro* and *in vivo* characterization of IIB-MEL LES-derived L2F6 and L3B9 clones with stable RNAi-mediated downregulation of SPARC expression. (A) Northern blot analysis of SPARC expression. Total RNA was extracted from L2F6, L3B9 clones and L-BLAST cell line, and SPARC mRNA levels were tested with a specific radioactive probe. Housekeeping gene 36B4 expression served as loading control. SPARC mRNA levels (3.0 and 2.1 kb transcripts) were dramatically diminished in L2F6, and slightly decreased in L3B9 cells. (B) *In vivo* subcutaneous tumor growth suppression of clones L2F6, L3B9 with stable expression of SPARC siRNA in athymic (*nude*) mice. Mice were injected subcutaneously in the left flank with 5×10^6 melanoma cells. Tumor volumes were determined as described in Materials and Methods. *Inset*: Photograph of subcutaneous tumor appearance in 3 mice treated with L-BLAST (left) and 3 mice treated with L2F6 (right) at the end of the experiment. (C) Immunoblotting detection of CLU, N-CAD and HSP27 in conditioned media of IIB-MEL LES-derived L2F6 and L3B9 clones and L-BLAST control cell line. Bars represent average of the relative optical densities of scanned immunoblotting bands corresponding to 3 biological replicates. Values were first normalized to optical densities corresponding to total protein loading. An unpaired ANOVA test with Dunnett post test was applied for statistical significance. A representative immunoblot image is shown for each protein below each plot, along with a representative loading control of total protein stained with Sypro Ruby (right).

secretion of HSP27. We confirmed that the three proteins are targets of SPARC by using three different strategies for knocking down SPARC expression in melanoma cells. Moreover, re-expression of SPARC reverted N-CAD, CLU, and HSP27 to levels close to those of control cells, indicating that their secretion is tightly regulated by SPARC. In the context of this work, we have also developed two new RNAi against SPARC. RNAi stably expressed in melanoma cells inhibited their *in vivo* growth confirming previous evidence that SPARC has a key role in promoting human melanoma tumorigenicity [13].

Invasion and spread of melanoma are related to alterations in cell adhesion [32]. Neural (N)-cadherin is a member of the cadherin family of transmembrane glycoproteins that mediate calcium-dependent, homotypic cell-cell adhesion. During melanoma progression to a more malignant phenotype, loss of functional epithelial (E)-cadherin (E-CAD) accompanies gain of expression of N-CAD [33–35]. This switch is part of the process of epithelial-mesenchymal transition seen during melanoma development that releases melanocytic cells from keratinocytes regulation [35]. Here, we found decreased levels both of membrane and soluble forms of N-CAD. Interestingly, shedding of the extracellular domain of N-CAD by proteolysis render a functional form of this protein [30]. Moreover, ADAM10-induced N-CAD cleavage resulted in changes in the cell adhesive behavior indicating that soluble N-CAD might greatly affect the migration and invasive capacity of tumor cells [28]. Recently, it was shown that SPARC overexpression induced a decrease in E-CAD levels in human primary melanocytes, leading to a promigratory and invasive behavior [36]. The functional relationship between SPARC and E-CAD was further confirmed in melanoma cells. Moreover, a very recent melanoma gene expression study showed a concomitant increase in SPARC and N-CAD in metastatic melanoma biopsies when compared with nonmetastatic melanoma [37]. Overall,

our study and the cited references strongly suggest that SPARC has a key role in epithelial-mesenchymal transition in melanoma development.

Among the other secreted proteins that were shown to be tightly regulated by SPARC we found clusterin (CLU). Human CLU is a highly *N*-glycosylated, secreted heterodimeric protein of 76–80 kDa that promotes cell survival while a second transcript coding for a smaller 50–55 kDa isoform has a nuclear localization and was described as proapoptotic [38, 39]. Recent results demonstrated that enhanced human colon cancer survival correlated with loss of the proapoptotic nuclear form of CLU and overexpression of its secreted form [40]. Overexpression of secreted CLU also appears to contribute to enhance bladder cancer cell survival and metastasic potential [41]. Accordingly, secreted CLU expression increased with melanoma progression from normal melanocytes to metastatic melanoma [42]. Interestingly, the possibility of SPARC acting on tumor cell apoptosis rendered conflicting evidence in other cancer types. In colon cancer, it was demonstrated that SPARC expression made cells sensitive to proapoptotic chemotherapeutic drugs [43]. Moreover, SPARC was shown to induce a proapoptotic effect in ovarian cancer [17]. In contrast, SPARC was shown to promote an antiapoptotic effect in glioma tumor cells through Akt activation [44]. Here, we observed that knock down of SPARC expression led to decreased levels of secreted CLU, leading us to hypothesize that SPARC might be protumorigenic at least in part by exerting a CLU-mediated antiapoptotic effect. However, we were unable to see any evidence of enhanced apoptosis in SPARC-deficient cells (data not shown), suggesting that CLU may mediate SPARC effects through additional pathways. Interestingly, secreted CLU and SPARC were shown to be coregulated in secretomes of Smad4(+) and Smad4(-) colon carcinoma cell lines [45, 46]. Moreover, TGFβ1 enhanced s-CLU protein and mRNA levels in a variety of cell types [47, 48]. The existence of a positive feedback loop between SPARC and TGFβ1 that was shown to affect tumor-stroma interaction [49–51], raises a potential link between SPARC, CLU, and TGFβ.

Although HSP27 is an intracellular protein, recent papers reported its extracellular release [52, 53]. HSP27 role in tumorigenesis is still controversial. In most cancer types, HSP27 was suggested to play a role as an antiapoptotic molecule [54]. In addition, overexpression of HSP27 increased the *in vivo* tumor aggressiveness in different models of colon and breast cancer [55, 56]. In contrast, overexpression of HSP27 was shown to inhibit the *in vitro* and *in vivo* aggressiveness of human melanoma cells [57]. Moreover, melanoma cells overexpressing HSP27 showed reduced cell invasiveness and decreased secretion of MMP-2 and MMP-9 [58]. These data clearly indicates an antitumorigenic role of HSP27 in melanoma which is consistent with the increased levels observed in melanoma cells with restricted SPARC expression. The lack of significant changes in HSP27 levels in cloned cells with restricted SPARC expression following RNAi expression is still unclear and remains open.

It is worth mentioning that only four out of the 13 identified differential proteins are classical secretion proteins (*i.e.*, CLU, SPARC, collagen I, collagen V). Among the rest, we found proteins from membrane, cytoplasmic or nuclear origin, in accordance with several other studies that describe secretomes [45, 46, 53, 59, 60]. One of the most interesting sources of secretion of intracellular content is the exosome [61]. Cytoskeletal proteins such as actin and tubulin, and several heat shock proteins including HSP27 [62] are contained in exosomal particles released into the extracellular medium by various cell types, including tumors, where they appear to be involved in tumor cell recognition by the immune system [63].

In summary, our results suggest that the concomitant decrease in the secreted levels of SPARC, N-CAD, and CLU, along with an increase in HSP27 levels may act synergistically in the abrogation of tumor progression. Our proteomics approach has proved to be a unique strategy to find SPARC-mediated molecular relationships that were not previously suggested by the literature. While it is difficult to anticipate the conveying molecular pathways, our findings, along with previous data from the literature, suggest that SPARC is a key element in the process of epithelial-mesenchymal transition that leads to increased melanoma growth and aggressiveness.

We wish to thank Lorena Benedetti for helping with animal studies, Emilio Camafeita for advice in mass spectrometry protein identification and Mariano Alvarez for running statistical analysis in R. This work has been supported in part by grants from the Agencia de Promoción Científica y Tecnológica (to O. L. P. and A. S. L.), Fundación Antorchas (to A. S. L.), and the Third World Academy of Sciences (to A. S. L.). We acknowledge the continuous support to O. L. P of Fundación René Baron and the Amigos de la Fundación Leloir para la Investigación en Cáncer (AFULIC).

5 References

[1] Brekken, R. A., Sage, E. H., SPARC, a matricellular protein: At the crossroads of cell-matrix communication. *Matrix Biol.* 2000, *19*, 569–580.

[2] Bradshaw, A. D., Sage, E. H., SPARC, a matricellular protein that functions in cellular differentiation and tissue response to injury. *J. Clin. Invest.* 2001, *107*, 1049–1054.

[3] Funk, S. E., Sage, E. H., The Ca^{2+}-binding glycoprotein SPARC modulates cell cycle progression in bovine aortic endothelial cells. *Proc. Natl. Acad. Sci. USA* 1991, *88*, 2648–2652.

[4] Funk, S. E., Sage, E. H., Differential effects of SPARC and cationic SPARC peptides on DNA synthesis by endothelial cells and fibroblasts. *J. Cell Physiol.* 1993, *154*, 53–63.

[5] Kupprion, C., Motamed, K., Sage, E. H., SPARC (BM-40, Osteonectin) inhibits the mitogenic effect of vascular endothelial growth factor on microvascular endothelial cells. *J. Biol. Chem.* 1998, *273*, 29635–29640.

[6] Sage, E. H., Vernon, R., Funk, S., Everitt, E., Angello, J., SPARC, a secreted protein associated with cellular proliferation, inhibits cell spreading in vitro and exhibits Ca^{2+}-dependent binding to the extracellular matrix. *J. Cell. Biol.* 1989, *109*, 341–356.

[7] Barker, T. H., Baneyx, G., Cardo-Vila, M., Workman, G. A., *et al.*, SPARC regulates extracellular matrix organization through its modulation of integrin-linked kinase activity. *J. Biol. Chem.* 2005, *280*, 36483–36493.

[8] Yan, Q., Sage, E. H., SPARC, a matricellular glycoprotein with important biological functions. *J. Histochem. Cytochem.* 1999, *47*, 1495–1506.

[9] Ledda, M. F., Bravo, A. I., Adris, S., Bover, L. *et al.*, The expression on the secreted protein acidic and rich in cysteine (SPARC) is associated with the neoplastic progression of human melanoma. *J. Invest. Dermatol.* 1997, *108*, 210–214.

[10] Rempel, S. A., Ge, S., Gutiérrez, J. A., SPARC: A potential diagnostic marker of invasive meningiomas. *Clin. Cancer Res.* 1999, *5*, 237–241.

[11] Bos, T. J., Cohn, S. L., Kleinman, H. K., Murphy-Ulrich, J. E. *et al.*, International Hermelin brain tumor symposium on matricellular proteins in normal and cancer cell-matrix interactions. *Matrix Biol.* 2004, *23*, 63–69.

[12] Sato, N., Fukushima, N., Maehara, N., Matsubayashi, H. *et al.*, SPARC/osteonectin is a frequent target for aberrant methylation in pancreatic adenocarcinoma and a mediator of tumor-stromal interactions. *Oncogene* 2003, *22*, 5021–5030.

[13] Ledda, M. F., Adris, S., Bravo, A. I., Kairiyama, C. *et al.*, Suppression of SPARC expression by antisense RNA abrogates the tumorigenicity of human melanoma cells. *Nat. Med.* 1997, *3*, 171–175.

[14] Woelfle, U., Cloos, J., Sauter, G., Riethdorf, L. *et al.*, Molecular signature associated with bone marrow micrometastasis in human breast cancer. *Cancer Res.* 2003, *63*, 5679–5684.

[15] Campo McKnight, D. A., Sosnoski, D. M., Koblinski, J. E., Gay, C. V., Roles of osteonectin in the migration of breast cancer cells into bone. *J. Cell Biochem.* 2005, *97*, 288–302.

[16] Mok, S. C., Chan, W. Y., Wong, K. K., Muto, M. G., Berkowitz, R. S., SPARC, an extracellular matrix protein with tumor-suppressing activity in human ovarian epithelial cells. *Oncogene* 1996, *12*, 1895–1901.

[17] Yiu, G. K., Chan, W. Y., Ng, S. W., Chan, P. S. *et al.*, SPARC (secreted protein acidic and rich in cysteine) induces apoptosis in ovarian cancer cells. *Am. J. Pathol.* 2001, *159*, 609–622.

[18] Chlenski, A., Liu, S., Crawford, S. E., Volpert, O. V. *et al.*, SPARC is a key Schwannian-derived inhibitor controlling neuroblastoma tumor angiogenesis. *Cancer Res.* 2002, *62*, 7357–7363.

[19] Alvarez, M. J., Prada, F., Salvatierra, E., Bravo, A. I. *et al.*, Secreted protein acidic and rich in cysteine produced by human melanoma cells modulates polymorphonuclear leukocyte recruitment and antitumor cytotoxic capacity. *Cancer Res.* 2005, *65*, 5123–5132.

[20] Kairiyama, C., Slavutsky, I., Larripa, I., Morvillo, V. *et al.*, Biologic, immunocytochemical, and cytogenetic characterization of two new human melanoma cell lines: IIB-MEL-LES and IIB-MEL-IAN. *Pigment Cell Res.* 1995, *8*, 121–131.

[21] Gorg, A., Obermaier, C., Boguth, G., Harder, A. *et al.*, The current state of two-dimensional electrophoresis with immobilized pH gradients. *Electrophoresis* 2000, *21*, 1037–1053.

[22] Heukeshoven, J., Dernick, R., Improved silver staining procedure for fast staining in phastSystem development unit. I. staining of sodium dodecyl sulfate gels. *Electrophoresis* 1988, *9*, 28–32.

[23] Shevchenko, A., Wilm, M., Vorm, O., Mann, M., Mass spectrometric sequencing of proteins silver-stained polyacrylamide gels. *Anal. Chem.* 1996, *68*, 850–858.

[24] Reed, L. J., Muench, H., A simple method of estimating fifty per cent endpoints. *Am. J. Hyg.* 1938, *27*, 493–497.

[25] Chomczynski, P., Sacchi, N., Single-step method of RNA isolation by acid guanidinium thiocyanate-phenol-chloroform extraction. *Anal. Biochem.* 1987, *162*, 156–159.

[26] Bradshaw, A. D., Reed, M. J., Sage, E. H., SPARC-null mice exhibit accelerated cutaneous wound closure. *J. Histochem. Cytochem.* 2002, *50*, 1–10.

[27] Bradshaw, A. D., Puolakkainen, P., Dasgupta, J., Davidson, J. M. *et al.*, SPARC-null mice display abnormalities in the dermis characterized by decreased collagen fibril diameter and reduced tensile strength. *J. Invest Dermatol.* 2003, *120*, 949–955.

[28] Reiss, K., Maretzky, T., Ludwig, A., Tousseyn, T. *et al.*, ADAM10 cleavage of N-cadherin and regulation of cell-cell adhesion and beta-catenin nuclear signalling. *EMBO J.* 2005, *24*, 742–752.

[29] Utton, M. A., Eickholt, B., Howell, F. V., Wallis, J., Doherty, P., Soluble N-cadherin stimulates fibroblast growth factor receptor dependent neurite outgrowth and N-cadherin and the fibroblast growth factor receptor co-cluster in cells. *J. Neurochem.* 2001, *76*, 1421–1430.

[30] Paradies, N. E., Grunwald, G. B., Purification and characterization of NCAD90, a soluble endogenous form of N-cadherin, which is generated by proteolysis during retinal development and retains adhesive and neurite-promoting function. *J. Neurosci. Res.* 1993, *36*, 33–45.

[31] Prada, F., Benedetti, L. G., Bravo, A. I., Alvarez, M. J. *et al.*, SPARC endogenous level, rather than fibroblast-produced SPARC or stroma reorganization induced by SPARC, is responsible for melanoma cell growth. *J. Invest. Dermatol.* 2007, DOI:10.1038/sj.jid.5700962, in press.

[32] Haass, N. K., Smalley, K. S., Li, L., Herlyn, M., Adhesion, migration and communication in melanocytes and melanoma. *Pigment Cell Res.* 2005, *18*, 150–159.

[33] Kuphal, S., Bosserhoff, A. K., Influence of the cytoplasmic domain of E-cadherin on endogenous N-cadherin expression in malignant melanoma. *Oncogene* 2006, *25*, 248–259.

[34] Silye, R., Karayiannakis, A. J., Syrigos, K. N., Poole, S. *et al.*, E-cadherin/catenin complex in benign and malignant melanocytic lesions. *J. Pathol.* 1998, *186*, 350–355.

[35] Li, G., Satyamoorthy, K., Herlyn, M., Dynamics of cell interactions and communications during melanoma development. *Crit. Rev. Oral Biol. Med.* 2002, *13*, 62–70.

[36] Robert, G., Gaggioli, C., Bailet, O., Chavey, C. *et al.*, SPARC Represses E-Cadherin and Induces Mesenchymal Transition during Melanoma Development. *Cancer Res.* 2006, *66*, 7516–7523.

[37] Alonso, S. R., Tracey, L., Ortiz, P., Perez-Gomez, B. *et al.*, A high-throughput study in melanoma identifies epithelial-mesenchymal transition as a major determinant of metastasis. *Cancer Res.* 2007, *67*, 3450–3460.

[38] O'Sullivan, J., Whyte, L., Drake, J., Tenniswood, M., Alterations in the post-translational modification and intracellular trafficking of clusterin in MCF-7 cells during apoptosis. *Cell Death Differ.* 2003, *10*, 914–927.

[39] Leskov, K. S., Klokov, D. Y., Li, J., Kinsella, T. J., Boothman, D. A., Synthesis and functional analyses of nuclear clusterin, a cell death protein. *J. Biol. Chem.* 2003, *278*, 11590–11600.

[40] Pucci, S., Bonanno, E., Pichiorri, F., Angeloni, C., Spagnoli, L. G., Modulation of different clusterin isoforms in human colon tumorigenesis. *Oncogene* 2004, *23*, 2298–2304.

[41] Miyake, H., Hara, I., Kamidono, S., Gleave, M. E., Synergistic chemsensitization and inhibition of tumor growth and metastasis by the antisense oligodeoxynucleotide targeting clusterin gene in a human bladder cancer model. *Clin. Cancer Res.* 2001, *7*, 4245–4252.

[42] Hoeller, C., Pratscher, B., Thallinger, C., Winter, D. *et al.*, Clusterin regulates drug-resistance in melanoma cells. *J. Invest Dermatol.* 2005, *124*, 1300–1307.

[43] Tai, I. T., Dai, M., Owen, D. A., Chen, L. B., Genome-wide expression analysis of therapy-resistant tumors reveals SPARC as a novel target for cancer therapy. *J. Clin. Invest.* 2005, *115*, 1492–1502.

[44] Shi, Q., Bao, S., Maxwell, J. A., Reese, E. D. *et al.*, Secreted protein acidic, rich in cysteine (SPARC), mediates cellular survival of gliomas through AKT activation. *J. Biol. Chem.* 2004, *279*, 52200–52209.

[45] Volmer, M. W., Radacz, Y., Hahn, S. A., Klein-Scory, S. *et al.*, Tumor suppressor Smad4 mediates downregulation of the anti-adhesive invasion-promoting matricellular protein SPARC: Landscaping activity of Smad4 as revealed by a "secretome" analysis. *Proteomics* 2004, *4*, 1324–1334.

[46] Volmer, M. W., Stuhler, K., Zapatka, M., Schoneck, A. *et al.*, Differential proteome analysis of conditioned media to detect Smad4 regulated secreted biomarkers in colon cancer. *Proteomics* 2005, *5*, 2587–2601.

[47] Wegrowski, Y., Perreau, C., Martiny, L., Haye, B. *et al.*, Transforming growth factor beta-1 up-regulates clusterin synthesis in thyroid epithelial cells. *Exp. Cell Res.* 1999, *247*, 475–483.

[48] Jin, G., Howe, P. H., Transforming growth factor beta regulates clusterin gene expression via modulation of transcription factor c-Fos. *Eur. J. Biochem.* 1999, *263*, 534–542.

[49] Reed, M. J., Vernon, R. B., Abrass, I. B., Sage, E. H., TGF-b 1 induces the expression of type I collagen and SPARC, and enhances contraction of collagen gels, by fibroblasts from young and aged donors. *J. Cell Physiol.* 1994, *158*, 169–179.

[50] Ford, R., Wang, G., Jannati, P., Adler, D. *et al.*, Modulation of SPARC expression during butyrate-induced terminal differentiation of cultured human keratinocytes: regulation via a TGF-beta-dependent pathway. *Exp. Cell Res.* 1993, *206*, 261–275.

[51] Bassuk, J. A., Pichler, R., Rothmier, J. D., Pippen, J. *et al.*, Induction of TGF-beta1 by the matricellular protein SPARC in a rat model of glomerulonephritis. *Kidney Int.* 2000, *57*, 117–128.

[52] Eustace, B. K., Sakurai, T., Stewart, J. K., Yimlamai, D. *et al.*, Functional proteomic screens reveal an essential extracellular role for hsp90 alpha in cancer cell invasiveness. *Nat. Cell Biol.* 2004, *6*, 507–514.

[53] Celis, J. E., Gromov, P., Cabezon, T., Moreira, J. M. *et al.*, Proteomic characterization of the interstitial fluid perfusing the breast tumor microenvironment: a novel resource for biomarker and therapeutic target discovery. *Mol. Cell. Proteomics* 2004, *3*, 327–344.

[54] Garrido, C., Schmitt, E., Cande, C., Vahsen, N. *et al.*, HSP27 and HSP70: potentially oncogenic apoptosis inhibitors. *Cell Cycle* 2003, *2*, 579–584.

[55] Garrido, C., Fromentin, A., Bonnotte, B., Favre, N. *et al.*, Heat shock protein 27 enhances the tumorigenicity of immunogenic rat colon carcinoma cell clones. *Cancer Res.* 1998, *58*, 5495–5499.

[56] Lemieux, P., Oesterreich, S., Lawrence, J. A., Steeg, P. S. *et al.*, The small heat shock protein hsp27 increases invasiveness but decreases motility of breast cancer cells. *Invasion Metastasis* 1997, *17*, 113–123.

[57] Aldrian, S., Trautinger, F., Frohlich, I., Berger, W. *et al.*, Overexpression of Hsp27 affects the metastatic phenotype of human melanoma cells in vitro. *Cell Stress Chaperones* 2002, *7*, 177–185.

[58] Aldrian, S., Kindas-Mugge, I., Trautinger, F., Frohlich, I. *et al.*, Overexpression of Hsp27 in a human melanoma cell line: regulation of E-cadherin, MUC18/MCAM, and plasminogen activator (PA) system. *Cell Stress Chaperones* 2003, *8*, 249–257.

[59] Gronborg, M., Kristiansen, T. Z., Iwahori, A., Chang, R. *et al.*, Biomarker discovery from pancreatic cancer secretome using a differential proteomics approach. *Mol. Cell. Proteomics* 2006, *5*, 157–171.

[60] Lafon-Cazal, M., Adjali, O., Galeotti, N., Poncet, J. *et al.*, Proteomic analysis of astrocytic secretion in the mouse: Comparison with the cerebrospinal fluid proteome. *J. Biol. Chem.* 2003, *278*, 24438–24448.

[61] Fevrier, B., Raposo, G., Exosomes: endosomal-derived vesicles shipping extracellular messages. *Curr. Opin. Cell. Biol.* 2004, *16*, 415–421.

[62] Clayton, A., Turkes, A., Navabi, H., Mason, M. D., Tabi, Z., Induction of heat shock proteins in B-cell exosomes. *J. Cell Sci.* 2005, *118*, 3631–3638.

[63] Thery, C., Zitvogel, L., Amigorena, S., Exosomes: composition, biogenesis and function. *Nat. Rev. Immunol.* 2002, *2*, 569–579.

